TLU 10/73

NONCOPLANAR PROTON CORRELATIONS FROM THE d(p,2p)n REACTION AT 10.00 MeV

B Sundqvist, A Johansson, L Gönczi and I Koersner

Tandem Accelerator Laboratory

Box 533

S-751 21 Uppsala, Sweden, tel 018/10 04 70

TLU 10/73
April 1973

NONCOPLANAR PROTON CORRELATIONS FROM THE d(p,2p)n REACTION AT 10.0 MeV

Bo Sundqvist, Arne Johansson, László Gönczi and Ib Koersner

Tandem Accelerator Laboratory, Uppsala, Sweden

ABSTRACT

Noncoplanar correlation spectra for the p + d breakup reaction have been measured at T_p = 10.0 MeV for 10 pairs of angles in a kinematically complete experiment. The kinematic conditions were chosen to enhance the "quasifree" reaction mechanism. The data have been parameterized with a cutoff radius by means of the MSIA (modified simple impulse approximation) model. The model was found to describe data rather well. For the largest angles (80° and 90°) between the scattering planes the experimental peak cross sections were found to be larger than the spectator model predictions (SIA), i.e.impossible to reproduce in the MSIA model with a positive cutoff radius.

This work was supported by the Swedish Atomic Research Council

1. INTRODUCTION

Deuteron breakup induced by neutrons or protons has been studied experimentally at various bombarding energies from a few MeV up to several hundred MeV[1]. The results have been analyzed with different approximate reaction models, for example the spectator model (quasifree-scattering) and the final-state interaction model. The common feature of these models is the assumption that a two-body process dominates the reaction mechanism. The procedure is to select data from a kinematic region where the model might be believed to be applicable. Consequently, information about the nucleon-nucleon interaction would be obtainable from such an analysis. For example, the Watson-Migdal theory for final-state interactions has been used in attempts to extract the n-n scattering length from data from the d(n,2n)p reaction[2].

Although Faddeev[3] formulated the integral equations for an exact solution of the three-body problem in the early sixties, it was not until recently that Amado[4], Cahill[5] and Ebenhöh[6], with the use of separable potentials, calculated the cross section for neutron and proton induced deuteron breakup by solving these equations. The separable potentials used were spin-dependent Yamaguchi interactions. Only s-wave interactions were used and the Coulomb potential was neglected, implying that, for the time being results from neutron induced deuteron breakup at low energy (T_n < 12 MeV) are the most relevant experimental data to test these calculations with. However, this experiment is difficult to perform with good accuracy and statistics due to the lack of intense, energetically and geometrically well defined, neutron beams and efficient neutron detectors. Few experiments of this kind have been made and data are very scarce. Furthermore, the n-n force is not known very well. Hopefully, Coulomb forces will be included in the calculations in the near future and the d(p,2p)n reaction data at low energy will then become an important test of the assumptions made about the nucleon-nucleon interactions used and the analysis might reveal the importance of off-energy-shell effects and three-body forces.

Therefore, it is an important task to measure d(p,2p)n cross sections for various kinematic situations. Until now only limited comparisons of d(p,2p)n reaction data with three-body theory have been made[6,7], a statement which is particularly true at low energies.

In a recent report from this laboratory[8] data for coplanar pp correlations from the d(p,2p)n reaction at 10.0 MeV incident proton energy were presented. The data were analyzed in terms of the modified simple impulse approximation (MSIA). As described by Johansson et al[9] the idea was to use this model to parameterize data and present them in a comprehensive form. The present work is an extension of that work to symmetric, noncoplanar correlations. As in the earlier experiment the directions and energies of two protons in coincidence were measured making the experiment kinematically complete. Apart from the fact that one reaches another part of phase space the noncoplanar correlations are interesting to use for a test of the quasifree picture. According to this model the process is most important for coplanar correlations and the noncoplanar behaviour is mainly determined by the deuteron wavefunction. Very few noncoplanar measurements have been reported for the d(p,2p)n reaction, only two measurements at 46 MeV incident proton energy, one for pp and the other for pn correlations[10,11]. Data in the present work were obtained at 10.0 MeV incident proton energy with the polar angles of the detectors kept at 30° and the angle between the scattering planes changed in steps of 10° between 0° and 90°. Some of the results have been reported earlier[12].

2. EXPERIMENTAL ARRANGEMENTS AND PROCEDURE

The experiment was performed with the Uppsala EN-tandem van de Graaff accelerator in a 38-cm-radius scattering chamber. A target of deuterated polyethylene was bombarded with a beam of 10.00 ± 0.01 MeV protons. The energies and directions of the two emerging protons were measured in coincidence using two surface barrier detectors, which defined small solid angles. The data i. e. the number of events as a function of the two proton energies, were stored in the memory of an on-line PDP-15 computer. The target structure changed in the beam and therefore protons elastically scattered from deuterium were counted in a separate monitor detector for the determination of absolute cross sections. The elastic pd data of Wilson et al[13] were used in the normalization. The experimental technique and apparatus have been described before[8] and only the details which were particular to this experiment will be mentioned here.

In the reaction studied

$$p + d \rightarrow p + p + n$$

the particles will be labelled with the indices 1, 2, 3, 4 and 5 from left to right in the following discussion.

One of the coincidence detectors (number 4), was kept fixed in the horizontal plane while the detector (number 3), which was moved, was put in a special holder placed on the second detector arm in the scattering chamber. This holder (Fig 1) made it possible to move the detector out of the scattering plane defined by the incoming beam and the fixed detector. In Fig 2 the notations used for the angles are defined. The experimentally convenient angles are called α and β and the ordinary spherical angles θ and φ. The horizontal plane of the scattering chamber is the x-z plane. β is the polar angle for the movable detector when in the horizontal plane, and this angle could be read from outside the chamber. The angle α could be read from a scale on the detector holder shown in Fig 1. The angles θ and φ are given by the equations below.

$$\theta = \arccos(\cos\alpha \cdot \cos\beta) \qquad (1)$$

$$\varphi = \operatorname{arctg}(\operatorname{tg}\alpha / \sin\beta) \qquad (2)$$

The accuracy of the setting of α was ± 0.3° and of β ± 0.1°. The corresponding uncertainties in θ and φ, listed in Table I, were estimated by differen-

tiating equations (1) and (2) and regarding the uncertainties in α and β as independent. The solid angles used and the corresponding angular resolutions are listed in Table II. The (azimuthal) angular resolution was rather bad but as can be seen from the results (Fig 14) it probably had no smoothening effect on the experimental data in the angular region studied.

In the experiment a beam current of 20-30 nA was used and the target was about 400 $\mu g/cm^2$. The beam spot diameter was smaller in this experiment than in the earlier one[8]. Two tantalum plates with circular holes (diameter = 1 mm) at the ends of a cylinder (800 mm long) defined the incoming beam. This meant that the maximum beam spot diameter at the target was 1.5 mm.

Due to the rather primitive detector holder used for the movable detector, the chamber had to be opened before every new spectrum measurement. However, the time needed to make the necessary changes from one spectrum to the start of a new one was about 1 hour, which was considered tolerably short compared to the time it took to accumulate one spectrum (5 hours).

The measurements covered symmetric, noncoplanar data with $\theta_3 = \theta_4 = 30^\circ$; $\varphi_4 = 180^\circ$; $\varphi_3 = 0^\circ - 90^\circ$ in steps of 10°. The spectra were taken on two occations and were obtained in the following order: $\varphi_3 = 30^\circ$, 20°, 10°, and 0°; $\varphi_3 = 0^\circ$, 40°, 60°, 50°, 70°, 80°, and 90°. The two measurements at $\varphi_3 = 0^\circ$ agreed within the statistical errors (Table III). Furthermore these measurements were also in fair agreement with corresponding measurement reported in ref 8.

A detailed account for the errors contributing to the uncertainty in the absolute cross section scale has been given[8]. The largest contribution to the total error came from solid angle uncertainties (about 2 %). The absolute scale was normalized to the same elastic pd cross section [13] as in ref 8 and consequently associated with the same uncertainties.

3. ANALYSIS AND DISCUSSION

In Fig 3-12 the projected correlation spectra are shown for the ten spectra (φ_3 = 0°, 10°, 20°, 30°, 40°, 50°, 60°, 70°, 80° and 90°). Fig 13 shows the cutoff radii extracted from the MSIA fits and the corresponding χ^2-values as functions of the angle between the scattering planes. In the fits all events corresponding to relative energies larger than 1 MeV for the two pn pairs possible were taken into account. The target thickness was corrected for as described in ref 6. As in the coplanar cases the fits are quite good. A summary of the results from the χ^2-fits is given in Table III. For φ_3 = 80° and 90° the simple plane-wave spectator model (MSIA with R_{co} = 0.0) gives peak cross sections which are equal to or smaller than the experimental values. In the corresponding spectra (Figs 11 and 12) the curves for R_{co} = 0 are shown. The fact that SIA gives a rather good description of the data at φ_3 = 80° is notable but probably accidental since for φ_3 > 70° the minimum neutron energy in the spectra is larger than 1 MeV and the neutron can hardly be regarded as a "spectator". Effects due to spectator protons should be included as well in those cases to make the model consistent.

The quasifree process is an approximate two-body process and should be more important for the coplanar case than in the noncoplanar case. The decrease of the peak cross section as a function of the angle between the scattering planes according to SIA is mainly determined by the square of the Fourier transform of the deuteron wave function. The φ_3 dependences of the free pp cross section used and of the phase space factor are rather slow (Fig 14).

In the analysis of the 46 MeV pp and pn noncoplanar data, Slaus et al[10] and Pettersen et al[11]) used a normalization constant to fit the SIA peak-value to the experimental result for the coplanar spectrum ($\theta_3 = \theta_4$ = 30° for the pp case and $\theta_3 = \theta_4$ = 45° for the pn case). Using the same normalization constant in SIA for the noncoplanar spectra they found that the experimental peak values fall below and above the theoretical curve in the p-p and p-n case, respectively. A similar analysis of the data in this work is shown in Fig 14. The experimental peak values were taken from the MSIA fits and for φ = 80° and φ = 90° weighted mean values for seven experimental points around the minimum neutron energy were used.

The experimental peak values are larger than the renormalized SIA curve at large angles between the scattering planes, in sharp contrast to the 46 MeV pp data. The renormalized SIA distribution describes the peak cross sections surprisingly well for small angles between the scattering planes.

However, the analysis shows the difficulties with the quasifree model to explain the noncoplanar experimental data both in absolute magnitude and in the variation with the angles between the scattering planes. It demonstrates the need of a more sophisticated theory where the interactions between all three nucleons are taken into account, as in the Faddeev equations[3].

Ebenhöh[6] has made such calculations using the separable potential approach. He explains the peak appearing at quasifree conditions as due to a backward peaking of the rearrangement amplitude for production of a pp pair. However, this explanation cannot hold for the peak observed at large angles between the scattering planes in the present experiment. Whereas the production angle for the correlated pair varies from 180° to about 140° from peak to half height of a coplanar "quasifree" peak, it only changes from 140° to 135° at $\varphi_3 = 60^{\circ}$.

REFERENCES

1. I Šlaus, Three Body Problem in Nuclear and Particle Physics, North Holland Publ Co, 1970 pp 337-389
2. B Zeitnitz, R Maschuw and P Suhr, Nucl Phys A 149 (1970) 449
3. L D Faddeev, Soviet Phys JETP 12 (1961) 1014
4. R Aaron and R D Amado, Phys Rev 150 (1966) 857
5. R T Cahill and I H Sloan, Nucl Phys A 165 (1971) 161
6. W Ebenhöh, Nucl Phys A 191 (1972) 97
7. H Klein, Dissertaion der Universität zur Köln, 1972(unpublished)
8. B Sundqvist, A Johansson, L Amtén, L Gönczi, I Koersner and B Palmgren, TLU 4/72, Tandem Laboratory Report, Uppsala 1972
9. A Johansson, B Sundqvist, L Gönczi and I Koersner, TLU 3/72, Tandem Laboratory Report, Uppsala 1972
10. I Šlaus, J W Verba, J R Richardson, R F Carlsson, L S August and E L Petersen, Phys Letters 23 (1966) 358
11. E L Pettersen, R Bondelid, P Tomaš, G Paić, J R Richardson and J W Verba, Phys Rev 188 (1969) 1497
12. A Johansson, B Sundqvist, L Amtén, L Gönczi, I Koersner and B Palmgren, Few Particle Problems in the Nuclear Interaction, North Holland/American Elsevier 1972, pp 491-494
13. A S Wilson, M C Taylor, J C Legg and G C Phillips, Nucl Phys A 130 (1969) 624

FIGURE CAPTIONS

Fig 1 Detector and collimator holder used for the detector moved out of the horizontal plane.

Fig 2 Coordinate system showing the experimental angles and the corresponding spherical angles.

Fig 3-10 Correlation spectra showing a projection of all the events on the energy axis of one of the protons. The solid lines are the MSIA fits to the experimental data between the two arrows.

Fig 11-12 Same as above but the solid line is the MSIA distribution with R_{co} = 0.0 fm.

Fig 13 Cutoff radii and χ^2-values for MSIA fits to noncoplanar reactions.

Fig 14 Experimental peak cross sections, the renormalized SIA distribution (N = 0.41), the square of the Fourier transform of the deuteron wave function, phase space factor and the free pp cross section used as a function of the angle between the scattering planes.

Table I Angular settings (α, β, θ, φ), uncertainties ($\Delta\theta$, $\Delta\varphi$) and resolutions ($\delta\varphi$) in the experiment. Notations are defined in Fig 2 (Quantities in degrees).

α	β	θ_3	φ_3	$\Delta\theta_3$	$\Delta\varphi_3$
0.0	30.0	30.0	0.0	0.1	0.6
5.0	29.6	30.0	10.0	0.1	0.6
9.9	28.5	30.0	20.0	0.1	0.6
14.5	26.6	30.0	30.0	0.2	0.5
18.7	23.9	30.0	40.0	0.2	0.5
22.5	20.4	30.0	50.0	0.2	0.4
25.7	16.1	30.0	60.0	0.3	0.4
28.0	11.2	30.0	70.0	0.3	0.3
29.5	5.7	30.0	80.0	0.3	0.2
30.0	0.0	30.0	90.0	0.3	0.2

$\theta_4 = 30^\circ$; $\varphi_4 = 180^\circ$; $\Delta\theta_4 = \pm 0.1$;

Ang. res; $\delta\varphi_4 = 3.4^\circ$; $\delta\varphi_3 = 4.3^\circ$ *

* FWHM in a distribution assuming circular distributions for detector aperture and beam spot.

Table II Solid angles used and their characteristics

Detector	Aperture diameter (mm)	Distance between target and collimator (mm)	Angular resolution* ($\delta\theta$)(deg)	Solid angle (msr)
3;movable	5.013 ± 0.002	80.0 ± 0.5	2.2	3.08 ± 0.04
4;fixed	5.007 ± 0.002	100.8 ± 0.5	1.7	1.95 ± 0.02
Monitor	5.020 ± 0.008	259.6 ± 0.5	0.7	0.294 ± 0.002

* FWHM in a distribution assuming circular distributions for detector aperture and beam spot.

Table III Summary of the results from the χ^2-fits.

Angle between scattering planes	Number of data points	$E^{min}_{neutron}$ (MeV)	Cutoff radius (fm)	$\sqrt{\chi^2}$	Remarks
0.0	19	0.058	$\begin{cases} 5.62 \pm 0.15 \\ 5.63 \pm 0.08 \end{cases}$	$\begin{cases} 1.45 \\ 1.12 \end{cases}$	5.63 ± 0.07
10.0	19	0.084	5.67 ± 0.14	1.53	
20.0	20	0.161	5.48 ± 0.14	1.50	
30.0	20	0.286	5.07 ± 0.10	1.28	
40.0	22	0.454	4.37 ± 0.06	1.06	
50.0	23	0.647	3.63 ± 0.07	1.07	
60.0	24	0.865	2.76 ± 0.07	0.93	
70.0	25	1.100	1.75 ± 0.12	1.38	$\sigma^{max} =$
80.0		1.330			2.41 ± 0.15
90.0		1.630			$\sigma^{max} =$ 2.51 ± 0.15

Fig 1

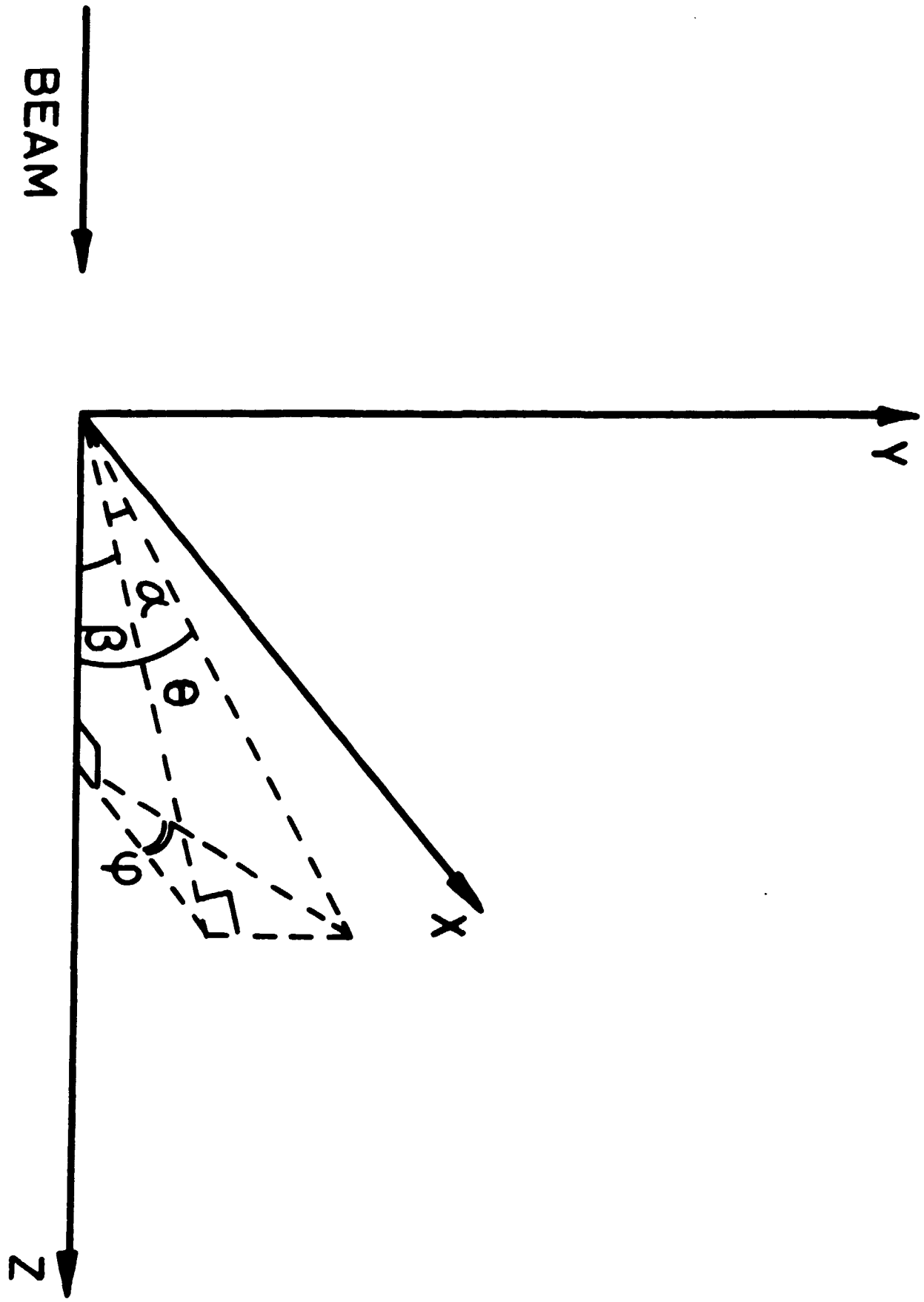

Fig 2

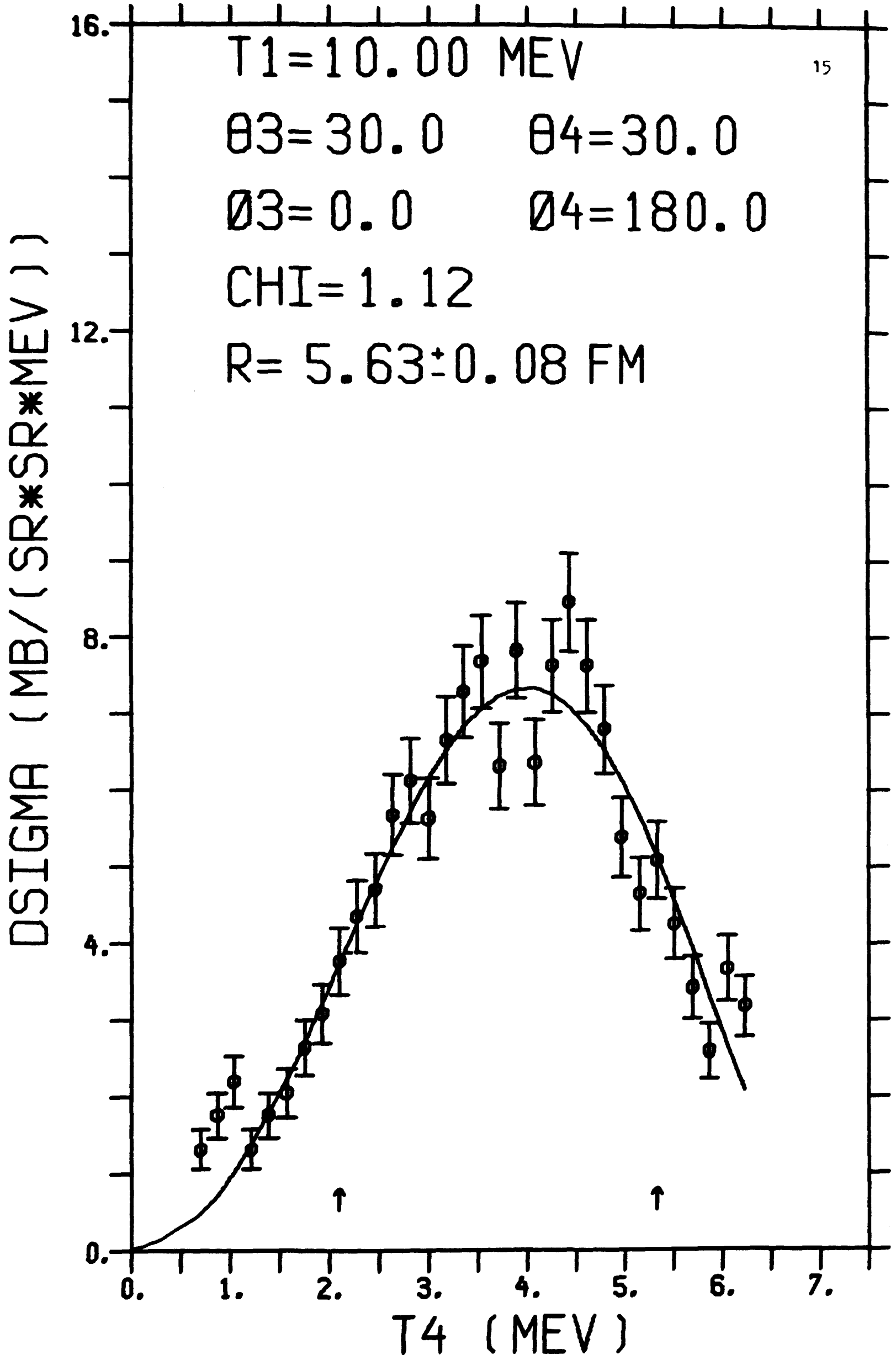
T1=10.00 MEV
θ3=30.0 θ4=30.0
Ø3=0.0 Ø4=180.0
CHI=1.12
R= 5.63±0.08 FM
DSIGMA (MB/(SR*SR*MEV))
T4 (MEV)
0.
4.
8.
12.
16.
0.
1.
2.
3.
4.
5.
6.
7.

Fig 3

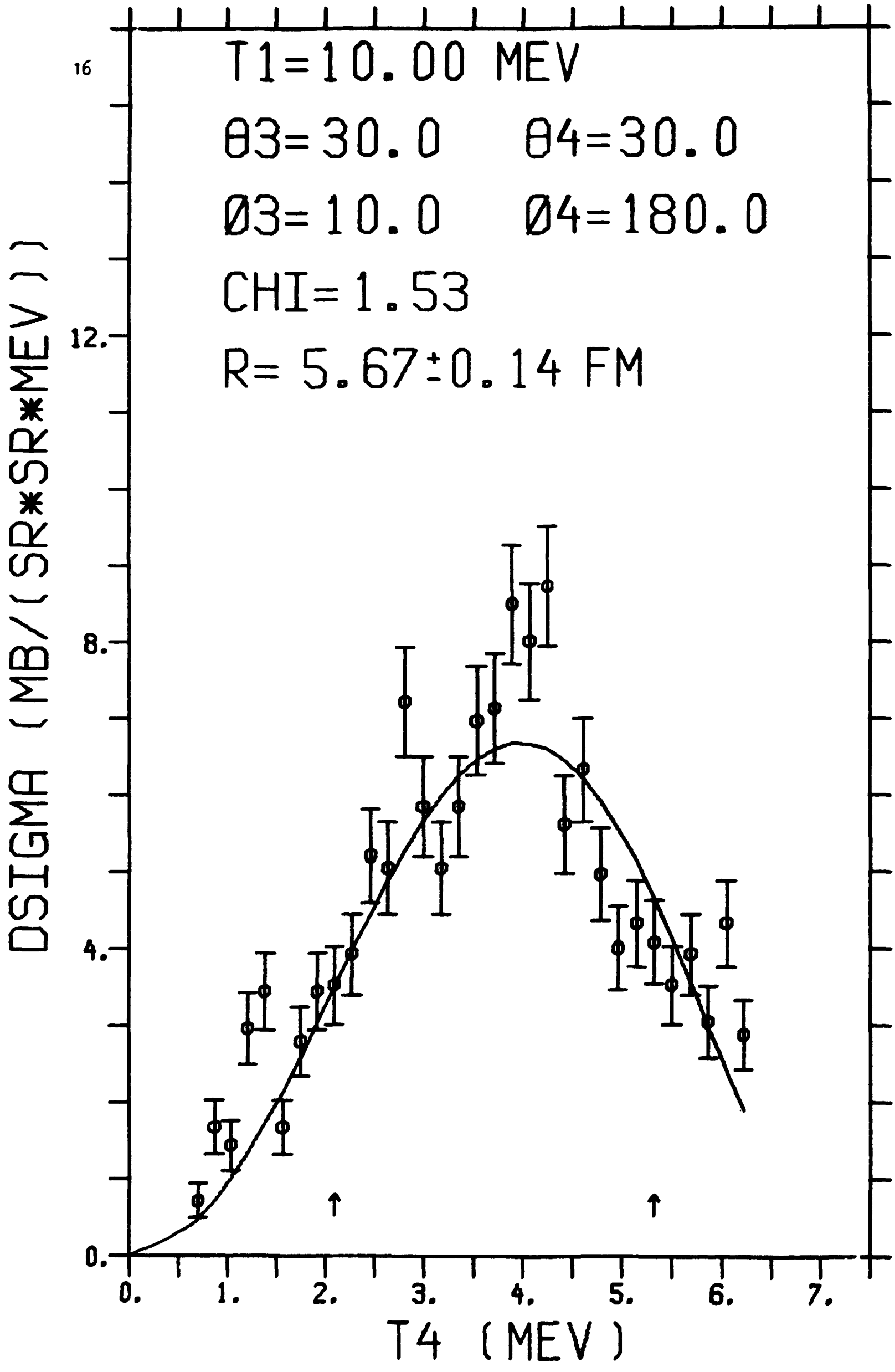
T1=10.00 MEV
θ3=30.0 θ4=30.0
Ø3=10.0 Ø4=180.0
CHI=1.53
R= 5.67±0.14 FM
DSIGMA (MB/(SR*SR*MEV))
16
12.
8.
4.
0.
0.
1.
2.
3.
4.
5.
6.
7.
T4 (MEV)

Fig 4

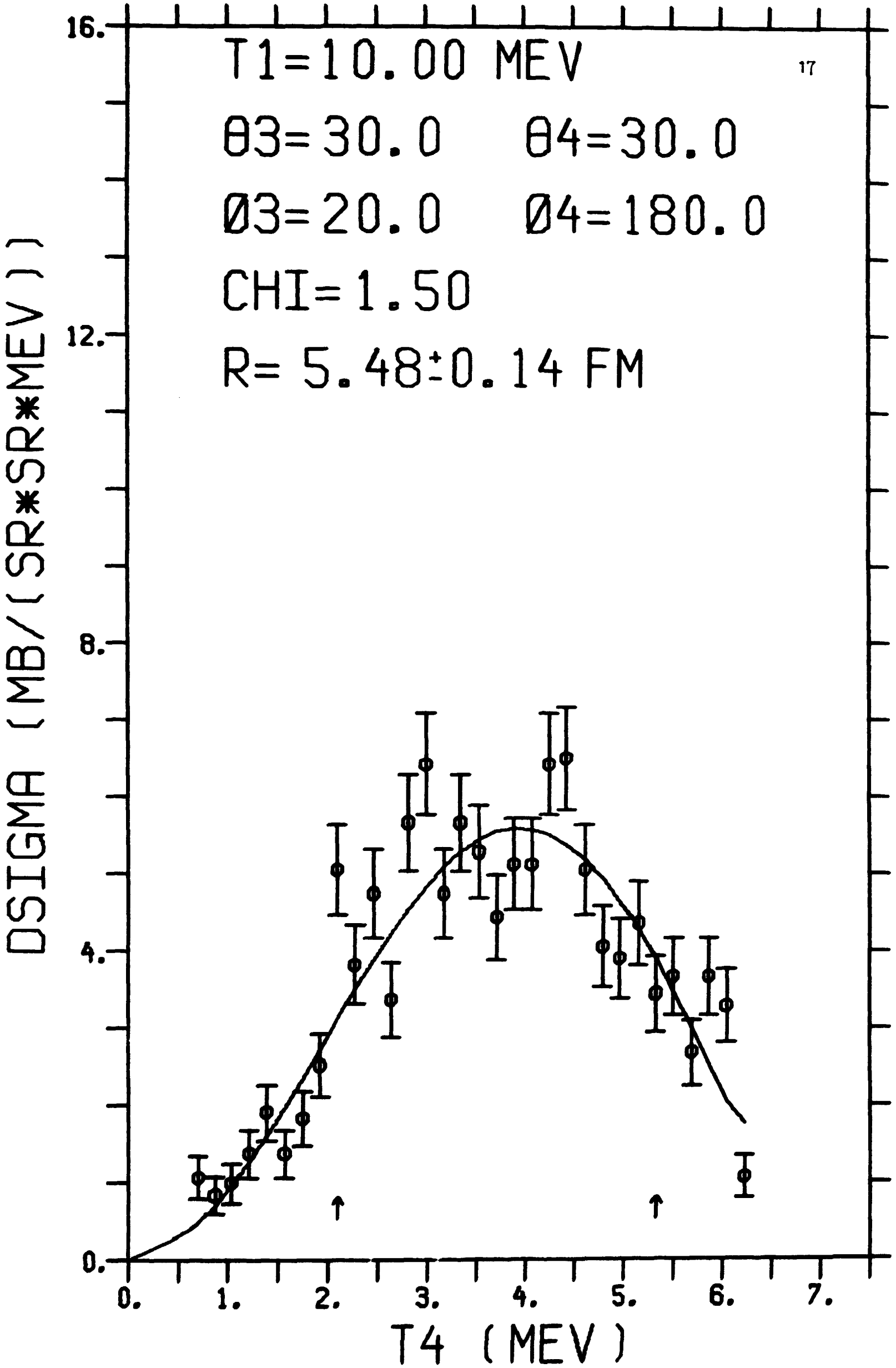
T1=10.00 MEV
θ3=30.0 θ4=30.0
Ø3=20.0 Ø4=180.0
CHI=1.50
R= 5.48±0.14 FM
DSIGMA (MB/(SR*SR*MEV))
T4 (MEV)
0.
4.
8.
12.
16.
0.
1.
2.
3.
4.
5.
6.
7.

Fir 5

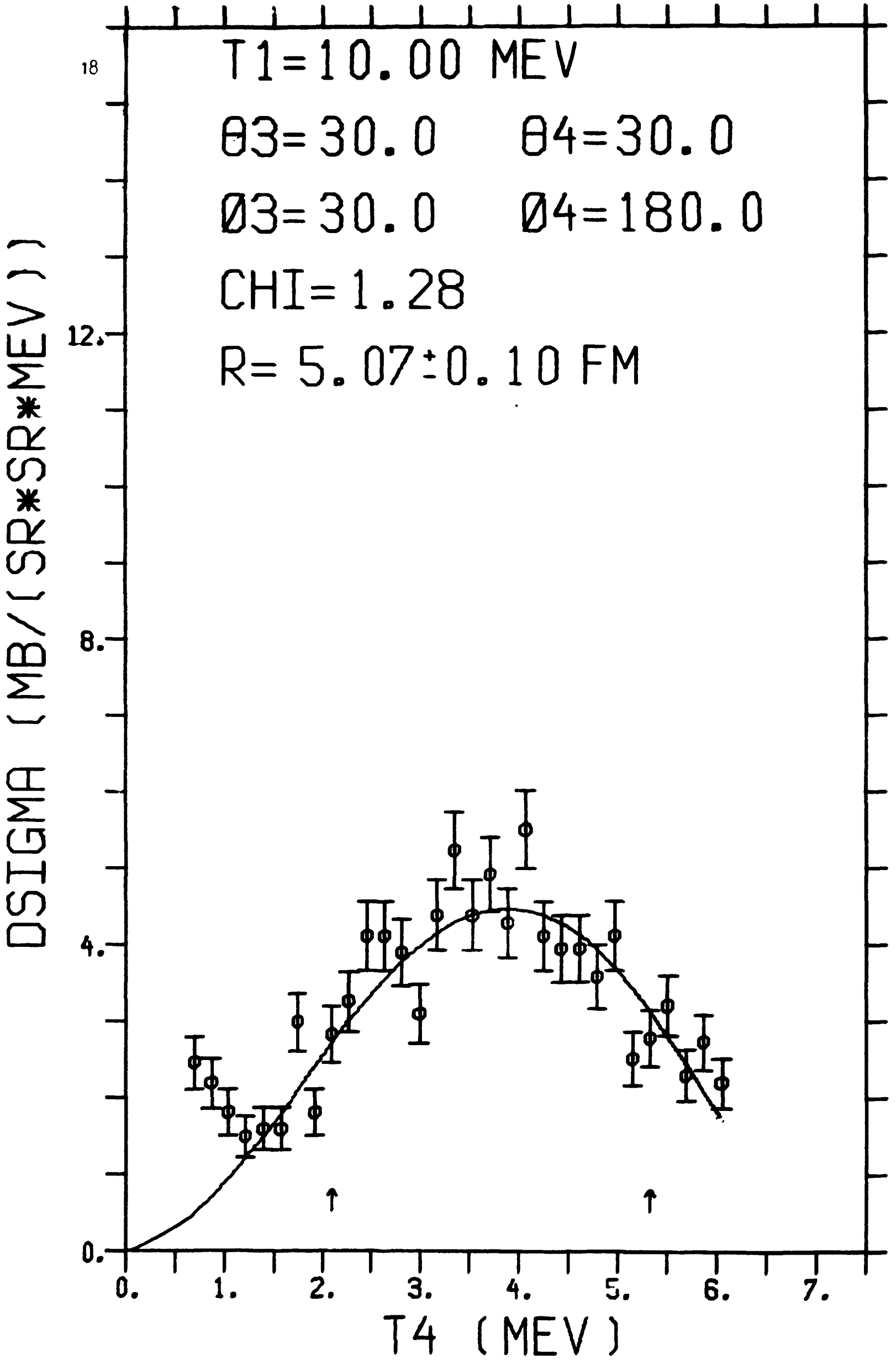
T1=10.00 MEV
θ3=30.0 θ4=30.0
Ø3=30.0 Ø4=180.0
CHI=1.28
R= 5.07±0.10 FM
DSIGMA (MB/(SR*SR*MEV))
18
12.
8.
4.
0.
0.
1.
2.
3.
4.
5.
6.
7.
T4 (MEV)

Fig 6

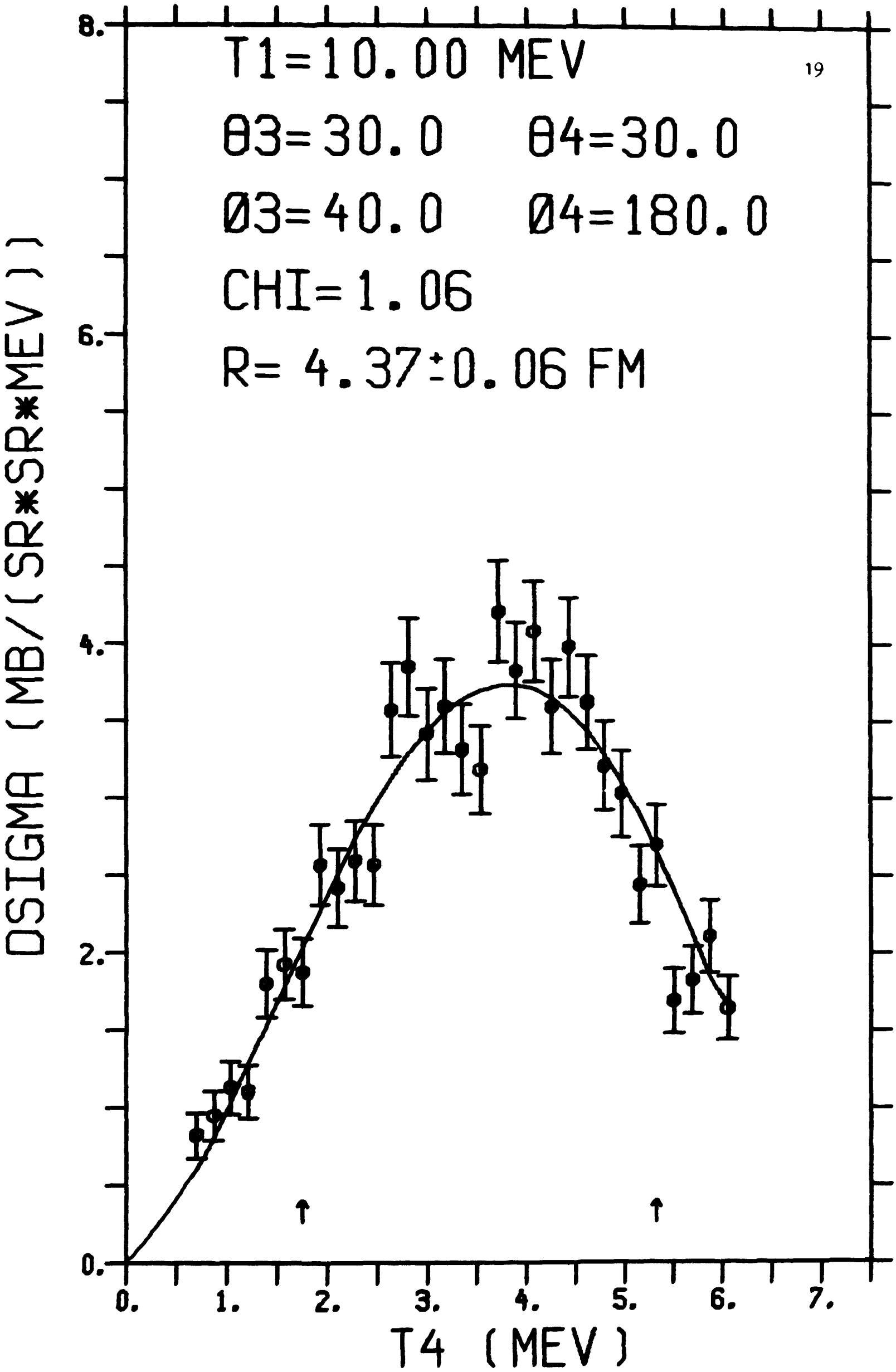
T1=10.00 MEV
θ3=30.0 θ4=30.0
Ø3=40.0 Ø4=180.0
CHI=1.06
R= 4.37±0.06 FM
DSIGMA (MB/(SR*SR*MEV))
T4 (MEV)
0.
2.
4.
6.
8.
0.
1.
2.
3.
4.
5.
6.
7.

Fig 7

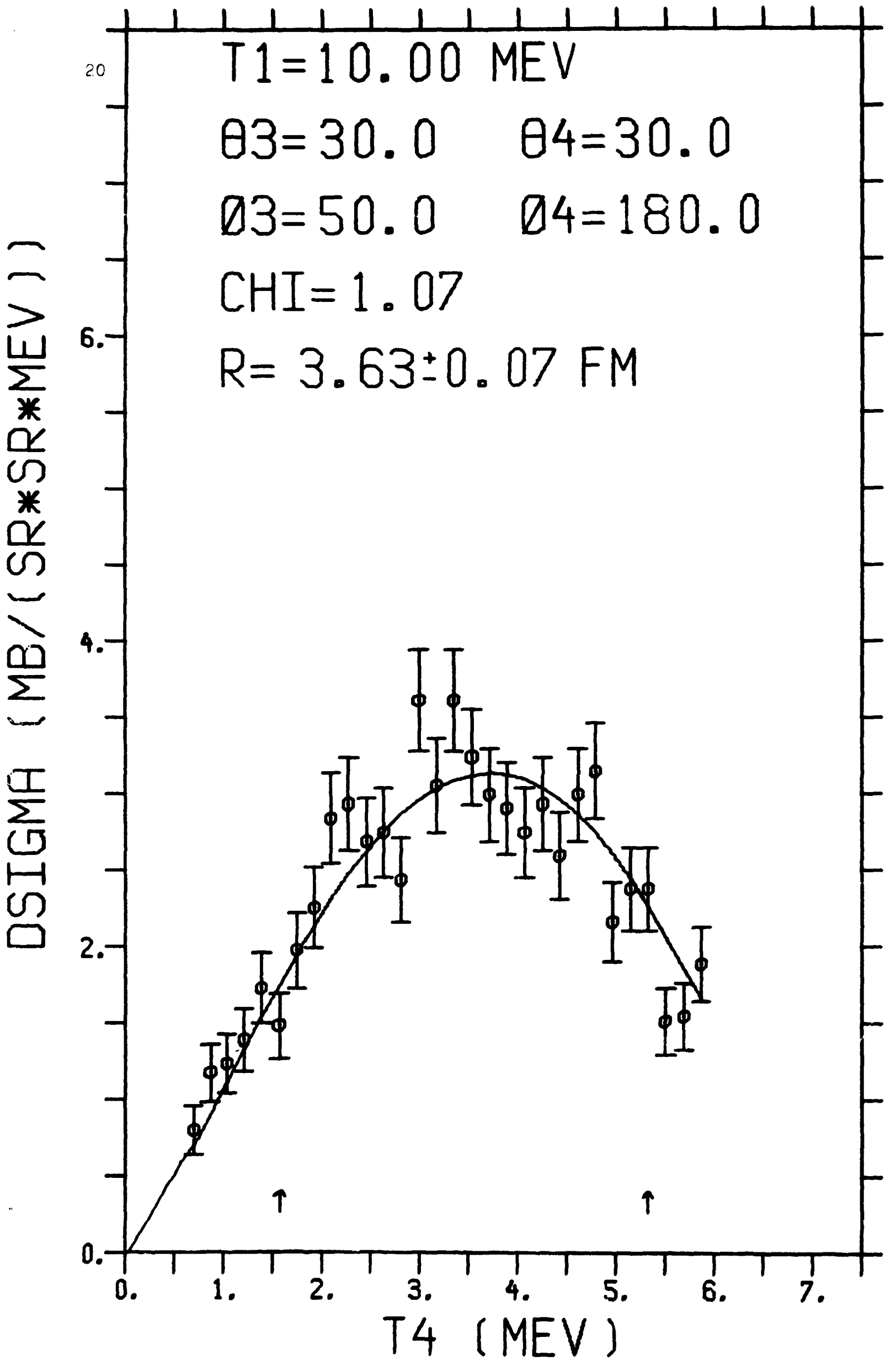
T1=10.00 MEV
θ3=30.0 θ4=30.0
Ø3=50.0 Ø4=180.0
CHI=1.07
R= 3.63±0.07 FM
DSIGMA (MB/(SR*SR*MEV))
T4 (MEV)
0.
2.
4.
6.
20
0.
1.
2.
3.
4.
5.
6.
7.

Fig 8

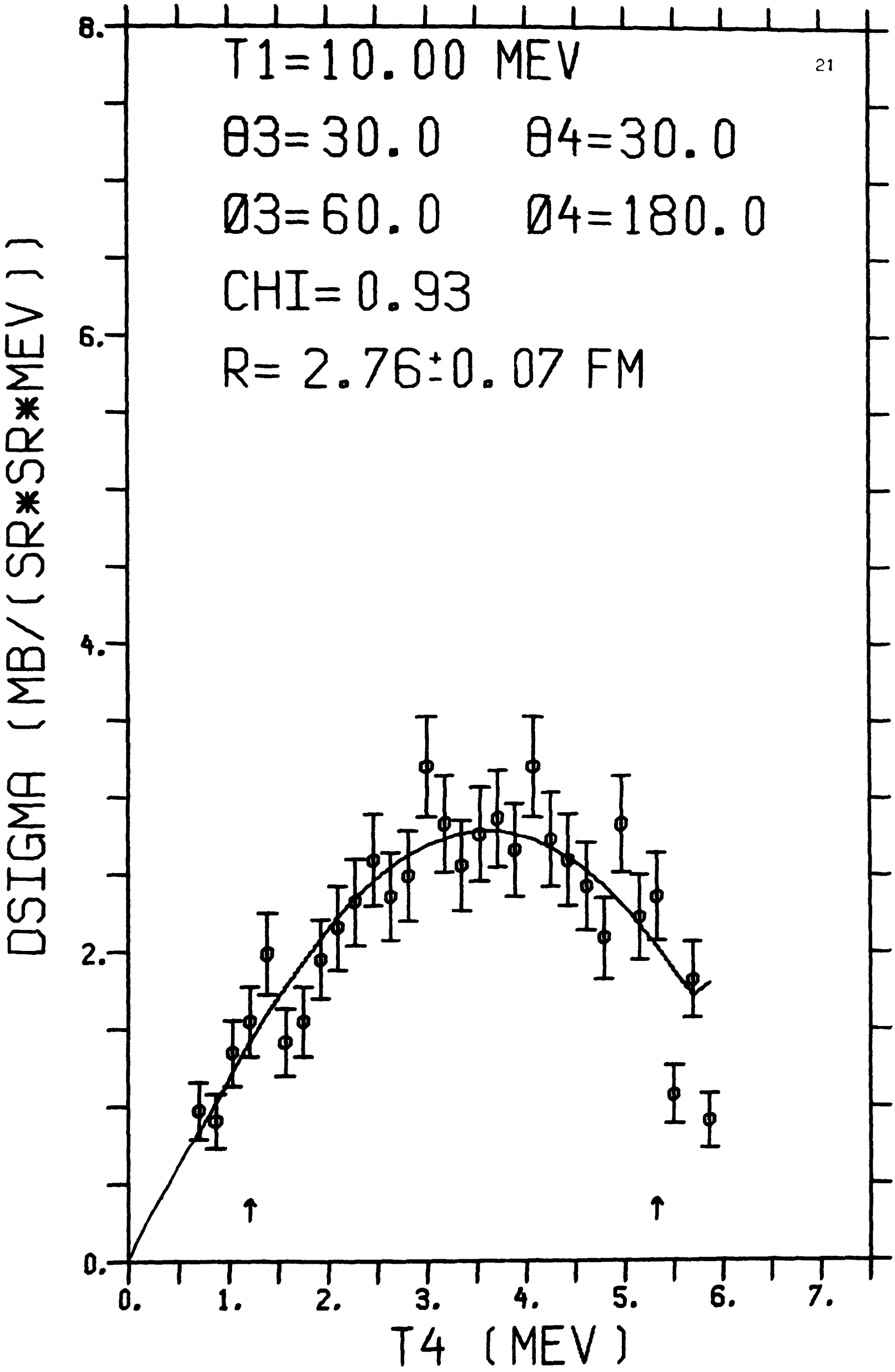
T1=10.00 MEV
θ3=30.0 θ4=30.0
Ø3=60.0 Ø4=180.0
CHI=0.93
R= 2.76±0.07 FM
DSIGMA (MB/(SR*SR*MEV))
T4 (MEV)
0.
2.
4.
6.
8.
0.
1.
2.
3.
4.
5.
6.
7.

Fig 9

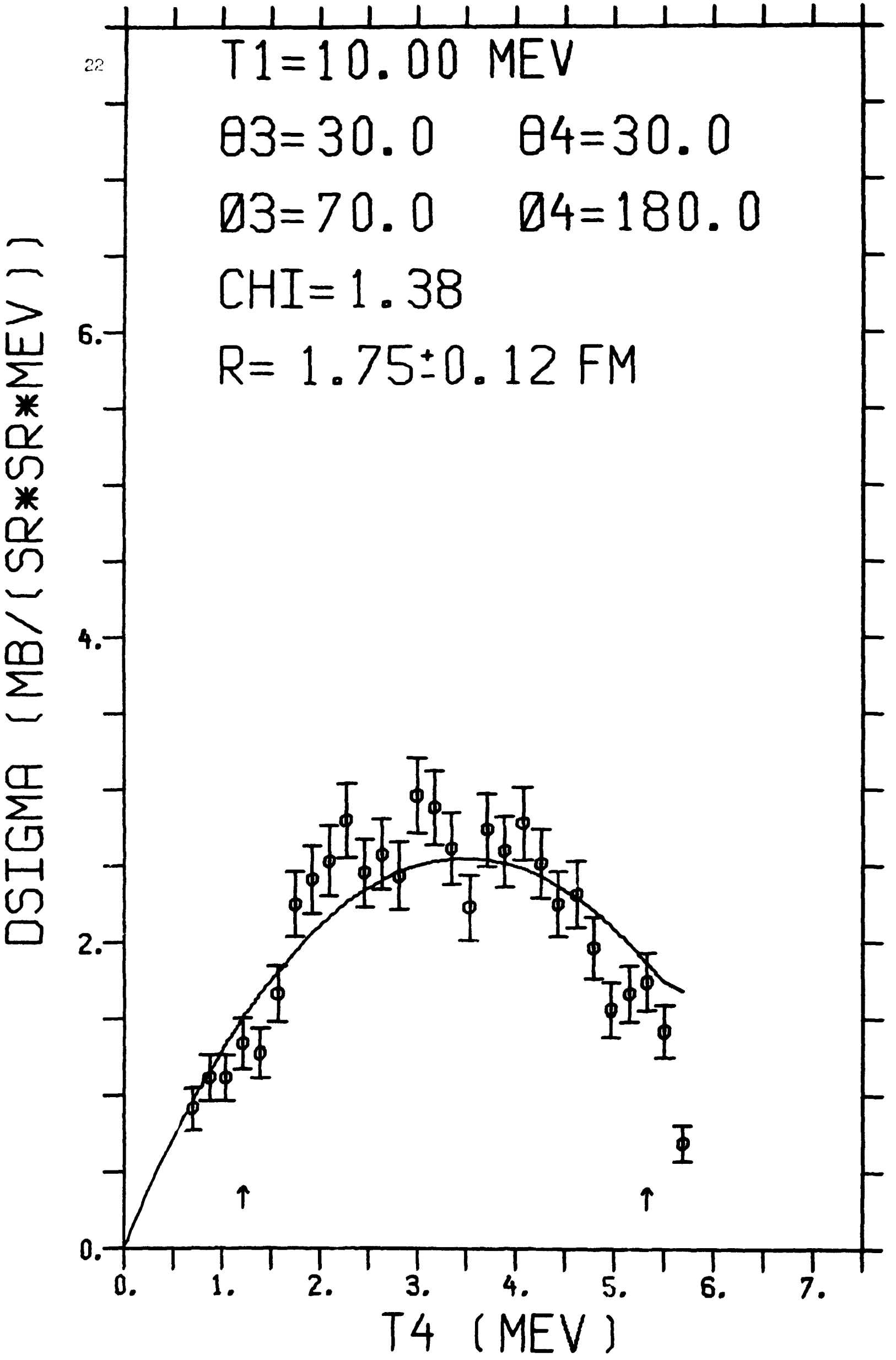
T1=10.00 MEV
θ3=30.0 θ4=30.0
Ø3=70.0 Ø4=180.0
CHI=1.38
R= 1.75±0.12 FM
DSIGMA (MB/(SR*SR*MEV))
T4 (MEV)
0.
2.
4.
6.
0. 1. 2. 3. 4. 5. 6. 7.

Fig 10

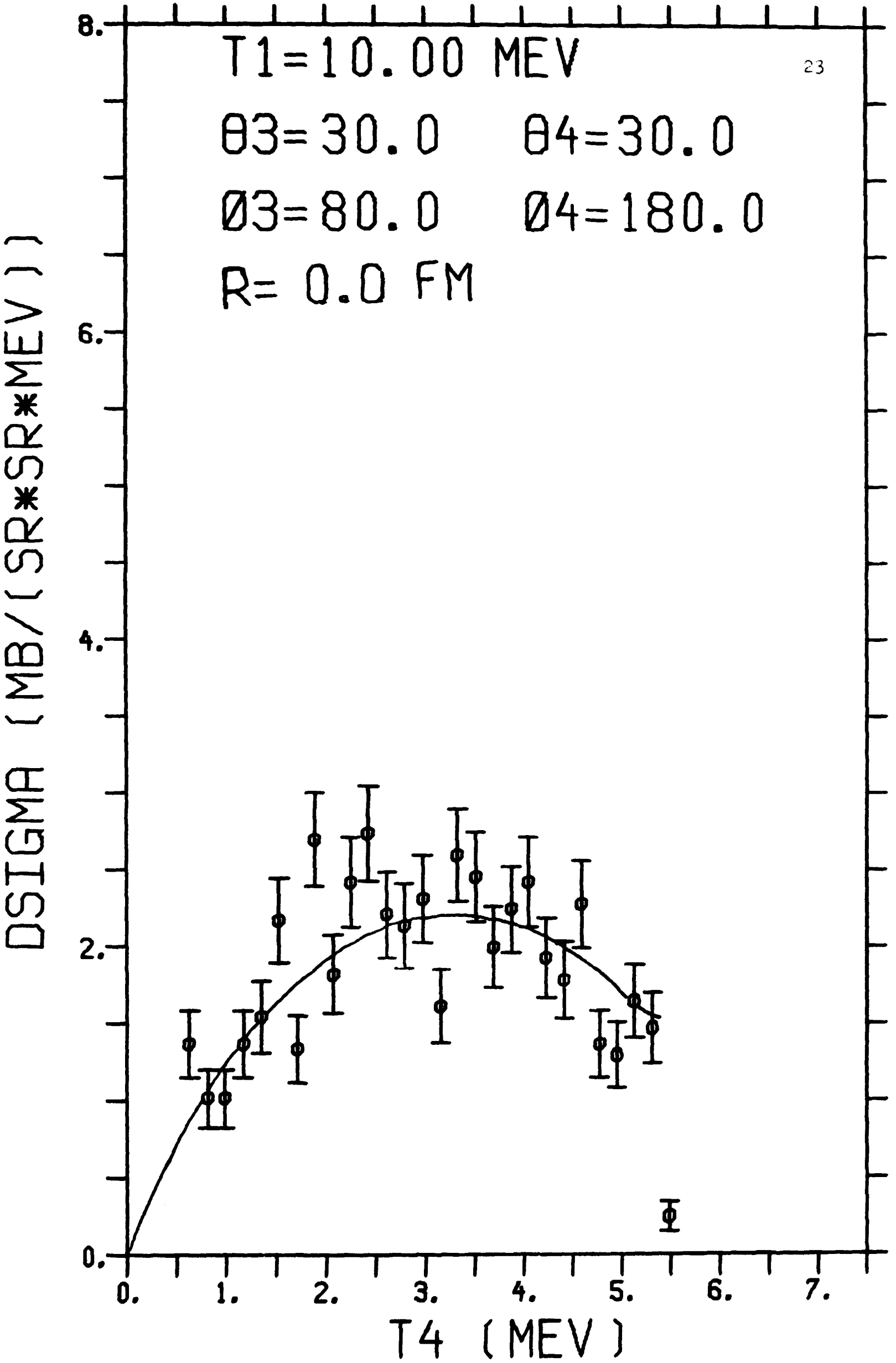
T1=10.00 MEV
θ3=30.0 θ4=30.0
Ø3=80.0 Ø4=180.0
R= 0.0 FM
DSIGMA (MB/(SR*SR*MEV))
T4 (MEV)
0.
2.
4.
6.
8.
0.
1.
2.
3.
4.
5.
6.
7.

Fig 11

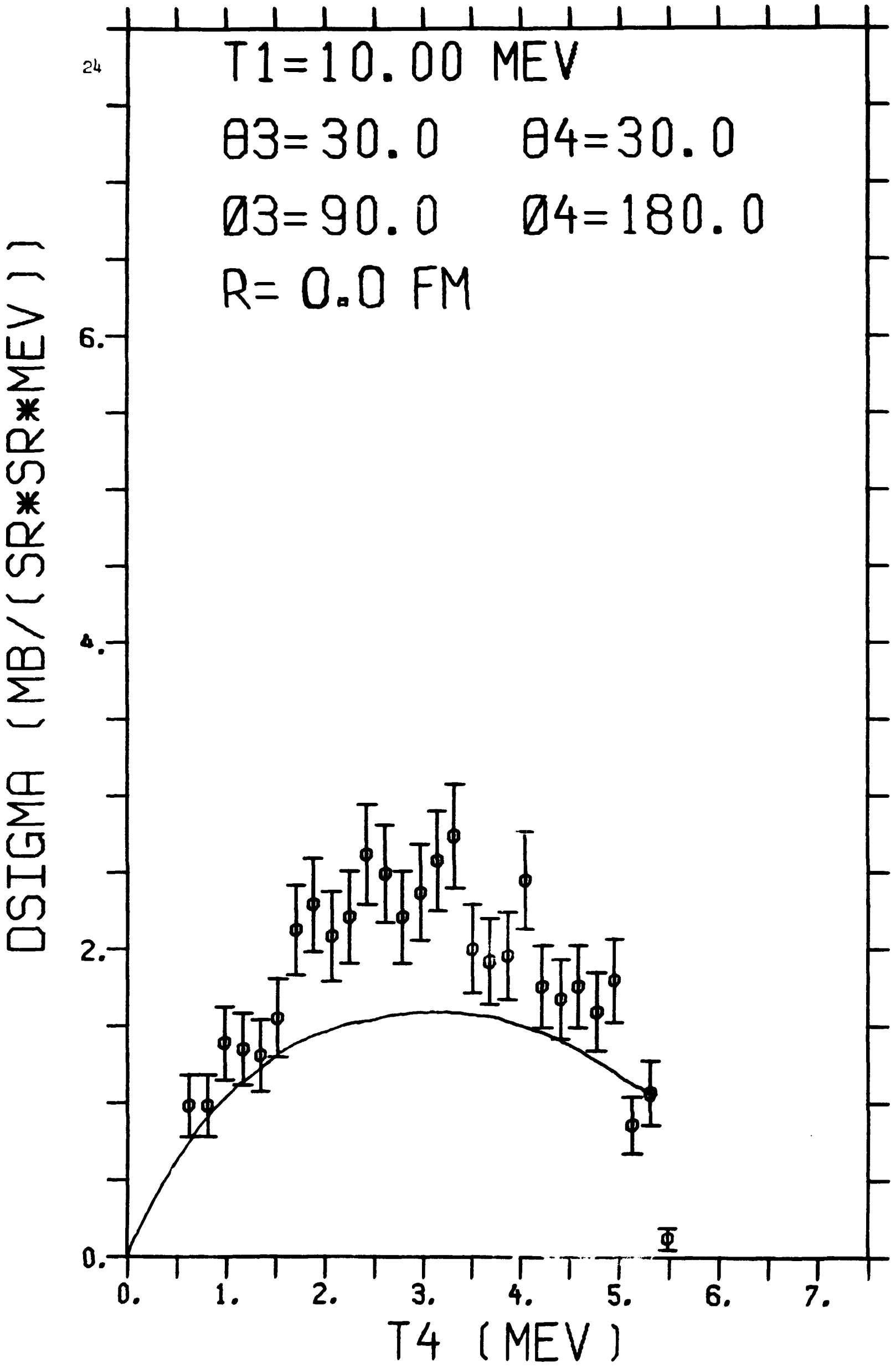
T1=10.00 MEV
θ3=30.0 θ4=30.0
Ø3=90.0 Ø4=180.0
R= 0.0 FM
DSIGMA (MB/(SR*SR*MEV))
24
6.
4.
2.
0.
0.
1.
2.
3.
4.
5.
6.
7.
T4 (MEV)

Fig 12

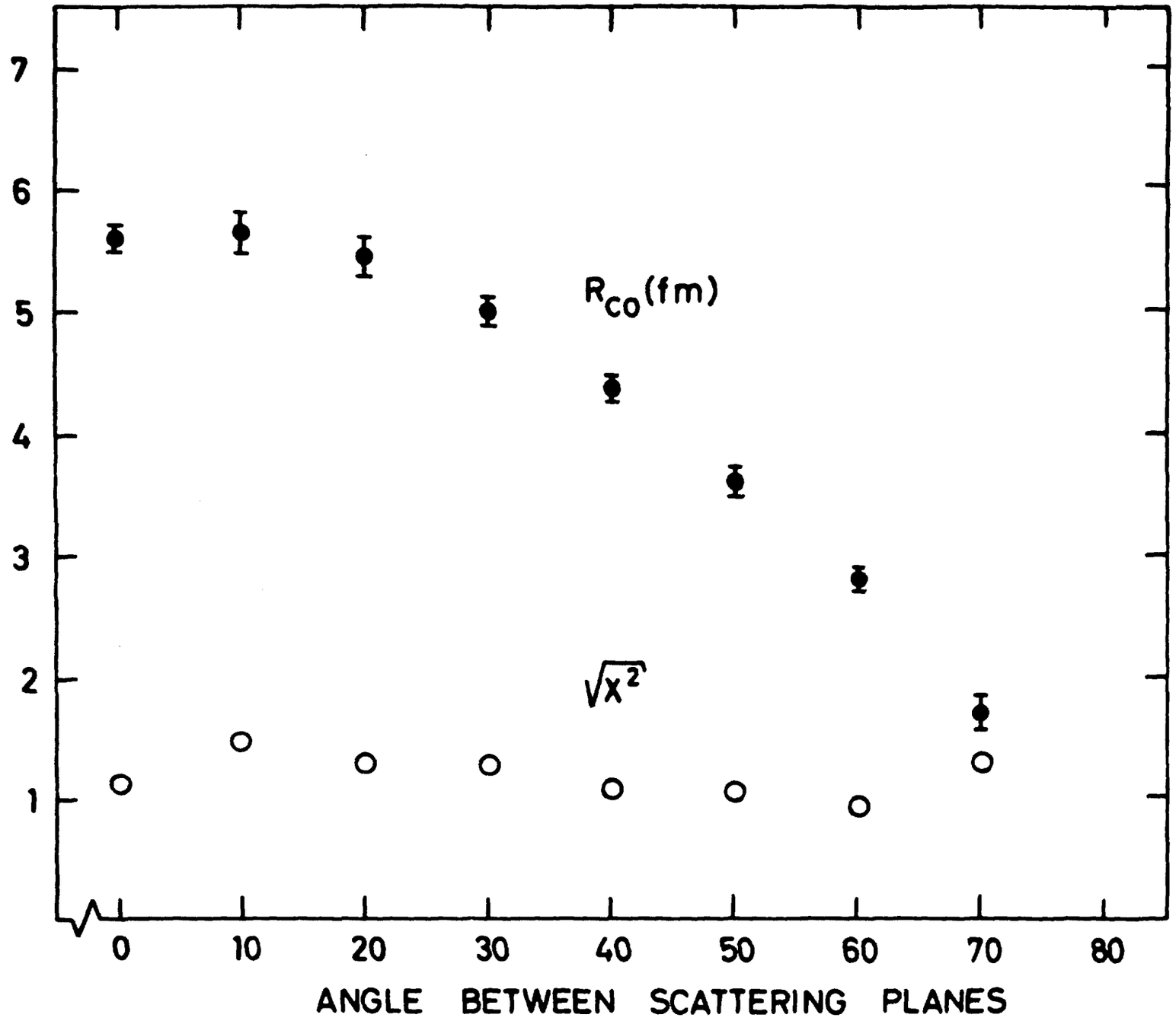
7
6
5
4
3
2
1
R_{co}(fm)
$\sqrt{X^2}$
0
10
20
30
40
50
60
70
80
ANGLE BETWEEN SCATTERING PLANES

Fig 13

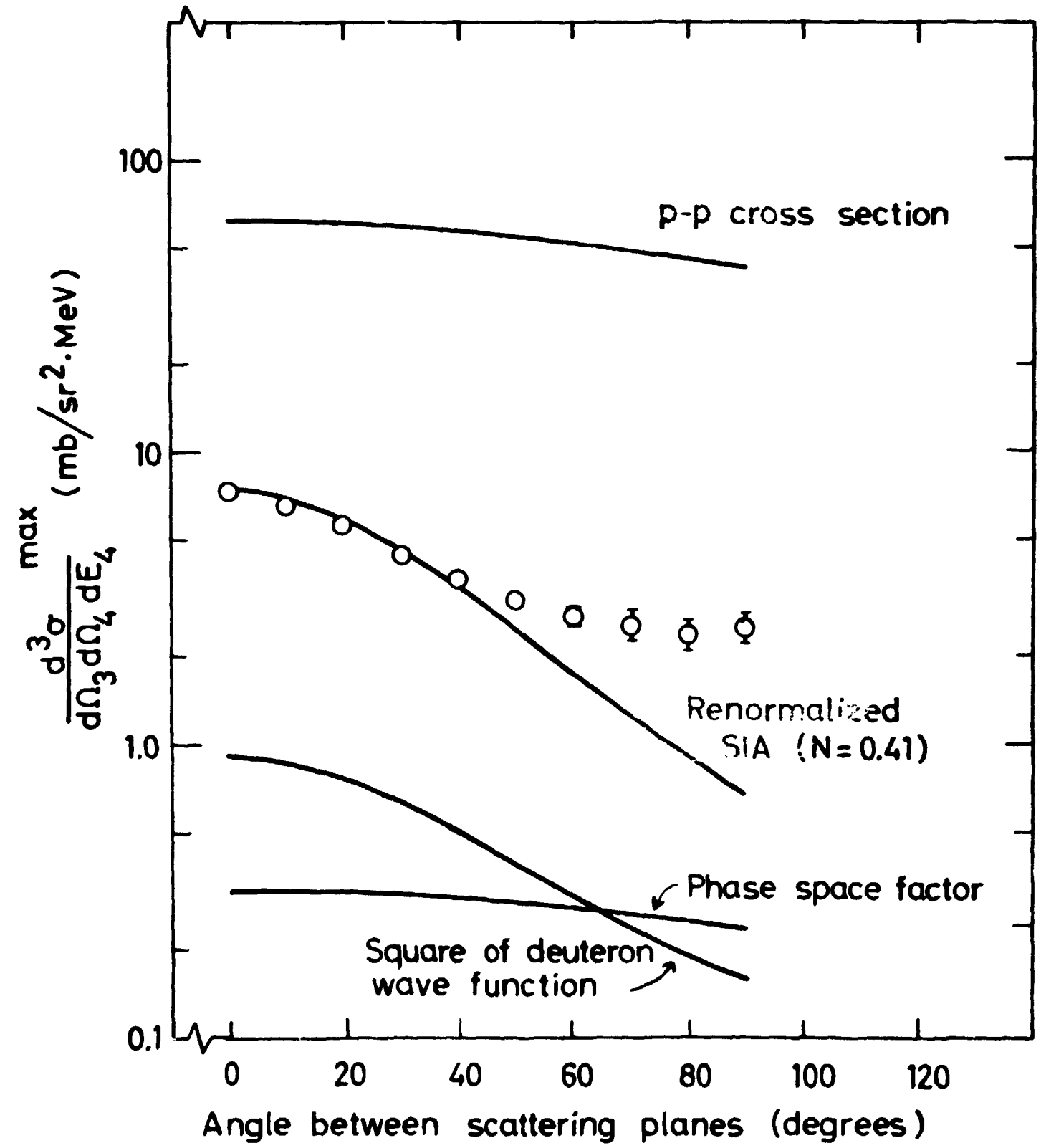
100
10
1.0
0.1
p-p cross section
Renormalized
SIA (N=0.41)
Phase space factor
Square of deuteron
wave function
0
20
40
60
80
100
120
Angle between scattering planes (degrees)
$\frac{d^3\sigma}{d\Omega_3 d\Omega_4 dE_4}\Big|_{max}$ (mb/sr^2.MeV)

Fig 14